Turkish Journal of Physics

Volume 38 | Number 2 Article 13

1-1-2014

UV-Vis and XRD investigation of graphite-doped poly(acrylic) acid membranes

MIHAI TODICA

TRAIAN STEFAN

SIMION SIMON

ISTVAN BALASZ

LIVIU DARABAN

Turkish Journal of Physics

http://journals.tubitak.gov.tr/physics/

Research Article

Turk J Phys
(2014) 38: 261 – 267

doi:10.3906/fiz-1305-16

UV-Vis and XRD investigation of graphite-doped poly(acrylic) acid membranes

Mihai TODICA*, **Traian STEFAN**, **Simion SIMON**, **Istvan BALASZ**, **Liviu DARABAN**

Condensed Matter Department, Faculty of Physics, "Babes-Bolyai" University, Cluj-Napoca, Romania

Received: 27.05.2013 • **Accepted:** 19.02.2014 • **Published Online:** 11.06.2014 • **Printed:** 10.07.2014

Abstract: Possible modification of the structure of poly(acrylic) acid (PAA) membranes doped with graphite was investigated by UV-Vis and XRD techniques. The pure PAA membranes were characterized by good transparency in the domain 250–700 nm, with maximum absorption at 207 nm. The absorbance of membranes increased significantly after doping with graphite. The XRD patterns of pure membranes showed a low degree of order of the polymeric matrix. Some modifications of the parameters of the ordered domains of the polymer and of the graphite appeared at high concentrations of the dopant.

Key words: Poly(acrylic) acid (PAA), graphite, structural modifications

1. Introduction

Polymeric membranes are used in different areas of human activities due to their special properties like high chemical stability, good flexibility and elasticity, low electric conductivity, and easy processing. Polymeric membranes are used in the pharmaceutical industry as support for active medical drugs, and most recently in the green energy industry in the fabrication of electric fuel cells based on the oxidation of methanol or hydrogen without burning [1–4]. The use of polymers like poly(vinyl) alcohol (PVA), and most recently poly(acrylic) acid (PAA), has increased for these purposes [5,6]. Such particular applications require special features of materials that are not characteristics of pure polymers as they result from the fabrication process, but can be obtained by doping with different inorganic compounds [7,8]. For instance, in the pharmaceutical industry, especially for products designed for skin care, the enhancement of UV protection is obtained by doping polymeric membranes with TiO_2 or graphite [9,10]. Doping with graphite allows the development of pharmaceutical products with controlled release of the active substance by electric fields. The release process can be activated by heating the polymeric support by weak electric currents, obtained from small electric sources, or induced by weak variable magnetic fields or microwaves of small intensity. This is the medical interest of doping the membranes with graphite. In the fabrication of electric direct methanol fuel cells (DMTF), which use Nafion membranes as separator, the diffusion of the fuel through the membrane is reduced by coating the membrane with PAA [11,12]. In both these applications, the introduction of graphite increases the electric conductivity of the polymer [13,14], but the addition of inorganic dopants could have an important influence on the microscopic physical properties of the polymeric matrix, modifications that can be investigated only by spectroscopic techniques. The aim of our study was the observation of possible modifications in the local structure of PAA induced by the addition of graphite to the polymeric matrix. These investigations were done by UV-Vis and XRD techniques.

*Correspondence: mihai.todica@phys.ubbcluj.ro

2. Materials and methods

The pure and doped membranes were obtained from aqueous PAA gel. The polymer in powder state was mixed in weight proportion of 10% with distilled water and stirred for 4 h at room temperature until a homogeneous gel was obtained. If no graphite is added, a transparent gel is obtained. This gel was displaying on glass plates and kept at room temperature until the water evaporated completely. The doped membranes were obtained from aqueous gel to which natural graphite was added at the desired concentration (5%, 15%, and 30%). The mixture was stirred for 3–4 h to ensure homogeneous dispersion of graphite into the polymeric matrix, at 40 °C, and then the compound was displayed on glass plates and kept in the dark at room temperature until the water evaporated. The UV-Vis investigation was done with a Jasco V-670 system with scan speed 200 nm/min, UV-Vis bandwidth 2 nm, and NIR bandwidth 8 nm. The X-ray diffraction (XRD) was performed with a Bruker X-ray diffractometer with Cu Kα ($\lambda = 0.154$ nm) at 45 kV and 40 mA. The 2θ range of 10°–100° was recorded with 0.1° steps.

3. Results and discussion

The first feature that changed after addition of graphite was the color of the sample. Before addition, the pure PAA membranes were colorless, being transparent for visible light. After addition of graphite, the color of samples changed progressively towards black and the transparence decreased significantly, being almost opaque at high graphite concentration. These modifications were observed by UV-Vis spectroscopy. The pure membrane showed good transparency in the domain 250–700 nm, with maximum absorption at 207 nm (Figure 1). As known from the literature, the absorption in the UV- Vis domain is determined by the excitation of the electrons from a full bonding or nonbonding orbital into an empty antibonding orbital [15,16]. These transitions appear in different domains of wavelength according to the atomic energy level difference involved. Usually the transitions of n or π electrons to the π^* excited state are the most studied because these transitions appear in an experimentally convenient region of the spectrum (200–700 nm). The absorption is proportional to the concentration of the absorber. In the PAA monomer, the absorption was determined mainly by the $\pi \rightarrow \pi^*$ transition of the carbonyl groups. These transitions were responsible for the absorption peak at 207 nm. After the addition of graphite, the absorption in the whole UV-Vis domain increased significantly. For instance, at 15% graphite concentration the absorbance increased by 70% compared with the absorbance at 5%, and at 30% graphite concentration the absorbance increased by 135% compared with the absorbance of the sample containing 5% graphite. However, the characteristic absorption peak of the PAA can be seen again in the spectra at the same wavelength as for the pure PAA membrane (Figure 1). The spectra of doped membranes appear as a superposition of the spectra of pure polymer and of pure graphite. The doped membranes combine the features of both components, but the optical properties of each component remain unaltered. From these observations it appears that the addition of graphite does not change the chemical structure of the polymer.

Another visible change that appears after doping is the brittleness of the samples. Before doping the polymeric membrane behaves like a flexible material, but as more graphite is added its flexibility decreases. Usually such modifications of the mechanical behavior can be correlated with changes in the crystallinity of the sample. The polymeric materials are known as amorphous systems, but in some cases the local parallel arrangement of the chains gives rise to ordered structures that behave like the atomic planes of the crystalline solid [17]. The interplanar distance is of the same order of magnitude as the wavelength of the X-rays. For a well-defined interplanar distance, as in the case of monocrystals, the observed diffraction peak is narrow and appears for a well-defined value of the diffraction angle θ according to Bragg's law, $k \cdot \lambda = 2 \cdot d \cdot \sin\theta$, where

k is the diffraction order, d the interplanar distance, and λ the wavelength of X radiation. In the polymers, the ordered domains are characterized by a multitude of these distances distributed around a value of higher probability. For each interplanar distance, Bragg's law is fulfilled for a well-defined value of the diffraction angle, giving rise to a narrow diffraction line. The observed diffraction signal is composed of these individual lines. As a consequence, the diffraction peak is broad, with a maximum corresponding to the most probable interplanar distance [15]. The area under the peak is proportional to the concentration of the corresponding ordered phase into the sample. This behavior can be seen from the diffractogram of pure PAA membrane. The diffractogram is characterized by an intense and broad signal at the angle of $2\theta = 17.2^\circ$ and a shoulder at $2\theta = 35^\circ$, in accord with other works [18] (Figure 2). This diffractogram is the result of the superposition of 2 peaks of diffraction that can be clearly seen only after simulation of the diffractogram. Each peak was approximated by Gaussian function centered on the diffraction angle, considering the amplitude and the width adjustable parameters. These parameters were modified until the best fit was obtained between the experimental and calculated data (Figure 2). The calculation of the parameters was done in the same conditions for all the samples in order to compare the numerical results. For a better analysis the simulated peaks are represented separately in Figure 2, as well as their convolution. From the diffraction angle we calculated the interplanar distances corresponding to each diffraction peak, d = 5.15 Å for $2\theta = 17.2^\circ$ and d = 2.5 Å for $2\theta = 35^\circ$. The interplanar distance d = 5.15 Å found for PAA is close to those obtained for other polymers with simple chemical structure, e.g., PVA, for which the interplanar distance is $\mathrm{d}_{PVA} = 5.51$ Å [19]. In PVA, the ordered phase is determined by the hydrogen bonds appearing between the OH groups of one monomer and the H atoms of the other monomer belonging to 2 neighboring chains, [20]. A similar process of packing of the chains appears in PAA [21]. Although the 2 polymers have very close chemical structures (Figure 3), the interplanar distances of PAA are greater due to the bending group COOH. The diffraction on different planes of PAA appears with different probabilities, which explains the difference between the amplitudes of the 2 peaks. The ratio of these probabilities is calculated from the ratio of the areas under the simulated peaks, $\mathrm{R}_{PAA} = 2.3$. The size of ordered domains was calculated with

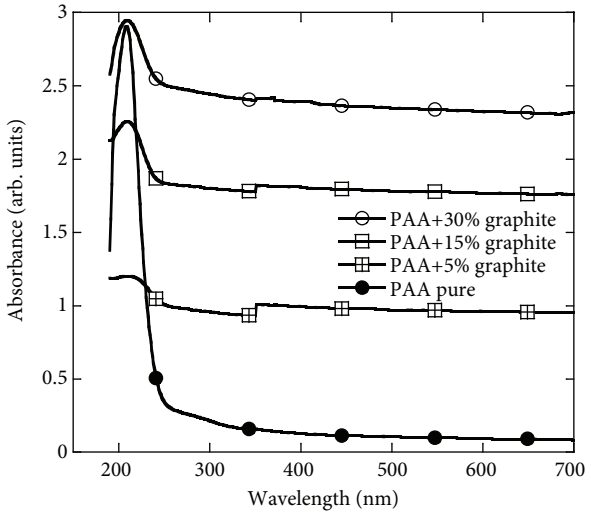

Figure 1. The UV-Vis absorbance of PAA membranes with different concentrations of graphite.

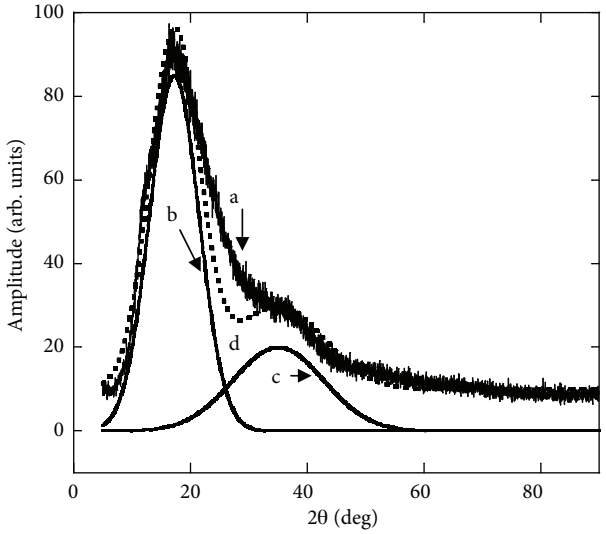

Figure 2. The XRD pattern of pure PAA membrane (a); the simulation of the peak at 17.2° (b); the simulation of the peak at 35° (c); the simulation of the whole spectrum (dashed line) (d).

the Debye–Scherrer equation applied to the simulated spectrum, $D = \frac{K \cdot \lambda}{\beta \cdot \cos\theta}$, where D is the size of ordered domains, $K = 0.9$ is a proportionality factor, and β the half line width of the peak expressed in radians. We obtained D = 8.9 Å. These observations show a low degree of crystallinity of the polymeric matrix before doping.

Our interest was to observe the modification of the ordered structure of the polymer after doping with graphite. For this purpose, the pure components and then the doped samples were investigated. Graphite represents 1 of the 4 allotropic forms of carbon, and consists of a hexagonal arrangement of carbon atoms in intercalated planes. In our experiments, the diffractogram of pure graphite contains 2 important peaks at $2\theta = 25.2^\circ$ and $2\theta = 43^\circ$, and a weak peak at $2\theta = 55^\circ$, which appear with different intensities (Figure 4). The interplanar distances corresponding to the first 2 peaks are d = 3.5 Å and d = 2.1 Å. The first peak corresponds to diffraction on the planes (002) and the second one to the planes (101) [22,23]. The (002) direction represents the c-axis of the graphite unit cell, which is perpendicular on the hexagonal planes. The peak at $2\theta = 55^\circ$ corresponds to the diffraction on planes (004) [24]. All the peaks are broad, but the characteristic parameters of each peak can be extracted from the simulation of data. The experimental data were simulated with a Gaussian function following the same algorithm of calculation that was utilized for the pure PAA. From the simulation we obtained the amplitude, the width, and the area under each peak, parameters that were used to calculate the size of the ordered domains and the probability of diffraction on the planes corresponding to each diffraction angle. For pure graphite the size of ordered domains is D = 22.6 Å and the ratio of probabilities of diffraction is $R_C = 10$.

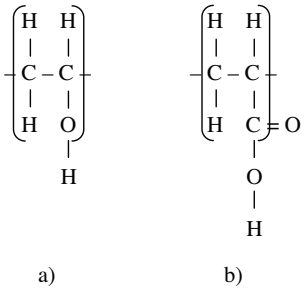

Figure 3. Chemical structure of PVA (a) and PAA (b) monomers.

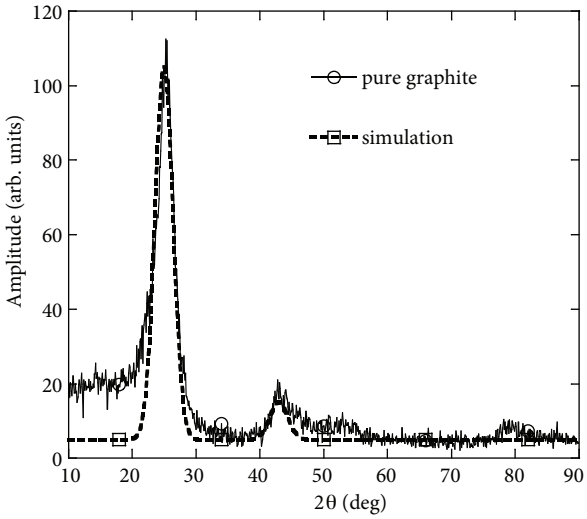

Figure 4. The XRD pattern of pure graphite (solid line) and the simulation of experimental data (dashed line).

Then we investigated the samples with graphite. The diffractograms of the doped membranes appear as a superposition of the spectra of the 2 components, as shown in Figure 5. Although the doped samples contain the characteristic diffraction peaks of the polymer and of the graphite, some modifications appear at high concentrations of dopant. For instance, at 30% graphite concentration, the first peaks of the PAA shift slowly from $2\theta = 17.2^\circ$ to $2\theta = 18.2^\circ$ and its half line width increases from 9° to 10°. That means a modification of interplanar distances from 5.15 Å to 4.86 Å and a modification of the size of ordered domains from 8.9 Å to 8.06 Å. The ordered domains of polymer become more compact in the presence of graphite. These results

suggest a repulsion of the polymeric chain from the graphite, forcing the polymer toward a more compact structure. The peak at $2\theta = 35^\circ$ is observed at the same angle; its half line width remains unchanged but its amplitude and its area increase. The ratio of areas under the 2 peaks of PAA became 1.2 (instead of 2.3 for pure membrane), indicating a decrease in probability of diffraction on the planes corresponding to the angle $2\theta = 18.2^\circ$. The peaks of graphite in the polymeric matrix appear at the same angles as for the pure state, indicating no modification of the interplanar distance. However, their amplitude and half widths are slowly modified. The half width of the peak at $2\theta = 25^\circ$ decreases slowly from 3.6° to 3.3° and the half width of the peak at $2\theta = 43^\circ$ decreases from 3.5° to 1.9°. That means a modification of the size of crystalline domains of graphite from D = 22.6 Å to D = 24.6 Å. The area under these peaks changes, the new ratio now being 13.3. That means an increase in the probability of diffraction on the planes (002) in the detriment of planes (101). The (002) direction becomes favorite in the presence of polymeric matrix. The values of these parameters show a high stability of the structure of graphite, referring especially to the interplanar distance, which is not modified by the presence of the polymer. However, a tendency of aggregation of graphite nanoparticles in domains with higher size as well as a preferential parallel alignment of the c axis of the hexagonal unit cells of graphite is observed in the presence of the polymeric matrix. Analysis of the features of all the peaks appearing in the diffractograms of doped samples was done on the basis of simulated spectra. An example of such a simulation, for the sample with 30% graphite, is presented in Figure 6. In this figure, each peak is represented separately and after superposition, with the amplitude and the width resulting from simulation.

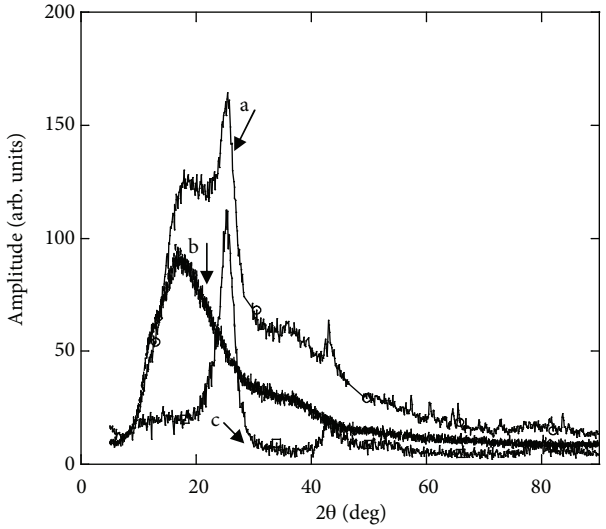

Figure 5. The XRD pattern of membrane PAA with 30% graphite (a); the XRD pattern of pure PAA membrane (b); the XRD pattern of pure graphite (c).

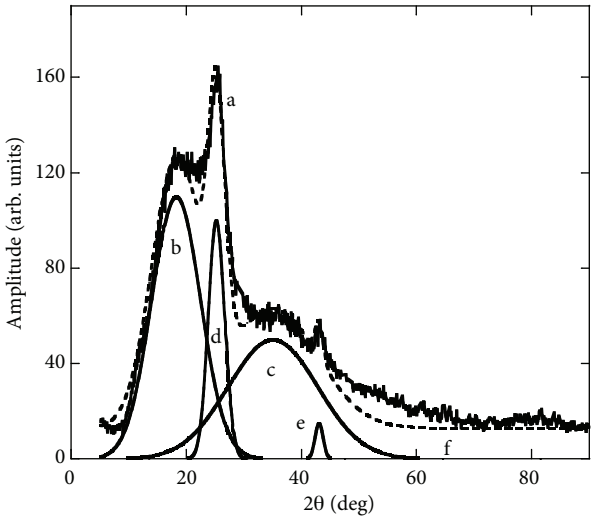

Figure 6. The XRD pattern of membrane PAA with 30% graphite (a); the simulation of the peaks of PAA at 18.2° (b) and at 35° (c); the simulation of the peaks of graphite at 25° (d) and at 43° (e); the simulation of the whole spectrum (f) (dashed line).

4. Conclusions

The absorption coefficient of pure PAA membranes in the domain 250–700 nm is almost constant, with a maximum at 207 nm. For the doped membranes the absorption increases progressively with the concentration of graphite in this domain, but the maximum at 207 nm of PAA can be seen again in these spectra. However, its

relative amplitude, compared with the amplitude in the domain 250–700 nm, decreases. This behavior indicates a superposition of the absorption properties of pure PAA and of graphite. The pure PAA membranes show a low degree of crystallinity determined by the local ordered arrangement of polymeric chains. The size of these ordered domains of the polymer decreases slowly after addition of graphite. We associate this behavior with a repulsive effect exerted by graphite nanoparticles upon the PAA chains. The diffraction peaks of graphite appear at the same angles in pure state as the doped samples, but the amplitude and the half width of some peaks are modified. Analysis of the parameters of these peaks indicates a small increase in the size of the crystalline phase of the graphite in the presence of polymeric chains and a preferential parallel alignment of the c axis of the unit cell of graphite. A tendency of aggregation of graphite nanoparticles in the presence of polymeric matrix is associated with this behavior.

Acknowledgments

This work was developed within the framework of the Sectorial Operational Program for Human Resources Development 2007–2013, POSDRU/107/1.5/S/76841 – "Innovative doctoral studies in a Knowledge Based Society", Babeş-Bolyai University, Cluj-Napoca, Romania, PhD scholarship granted to Traian Stefan; and CNCSIS-UEFISCDI, project PNII – ID_PCCE_101/2008.

References

[1] Hoffman, A. S. *Adv. Drug Del. Rev.* **2002**, *43*, 3–12.

[2] Sriamornsak, P.; Kennedy, R. A. *Int. J. Pharm.* **2006**, *323*, 78–83.

[3] Baglio, V.; Arico, A. S.; Blasi, A. D.; Antonucci, V.; Antonucci, P. L.; Licoccia, S.; Traversa, E.; Fiory, F. S. *Electochim. Acta* **2005**, *50*, 1241–1246.

[4] Deivaraj, T. C.; Lee, J. Y. *J. Power Sources* **2005**, *142*, 43–49.

[5] Todica, M. *Chin. Phys. Lett.* **2008**, *25*, 2674–2676.

[6] Todica, M.; Pop, C. V.; Udrescu, L.; Pop, M. *Chin. Phys. Lett.* **2010**, *27*, 018301-1-018301-4.

[7] Yang, C. C.; Lee, Y. J.; Yang, J. M. *Journal of Power Sources* **2009**, *188*, 30–37.

[8] Yang, C. C. *Journal of Membrane Science* **2007**, *288*, 51–60.

[9] Ruixia, H.; Leigang, W.; Jin, W.; Nan, H. *Applied Surface Science* **2010**, *256*, 5000–5005.

[10] Gambichler, T.; Tomi, N. S.; Moussa, G.; Huyn, J.; Dickel, H.; Altmeyer, P.; Kreuter, A. *J. Am. Acad. Dermatol.* **2006**, *55*, 882–885.

[11] Mallakpour, S.; Barati, A. *Progress in Organic Coatings* **2011**, *71*, 391–398.

[12] Thangamuthu, R.; Lin, C. W. *J. Power Sources* **2005**, *150*, 48–56.

[13] Ui, C.; Kikuchi, S.; Mikami, F.; Kadoma, Y.; Kumagai, N. *J. Power Sources* **2007**, *173*, 518–521.

[14] Sun, Z.; Yuan, A. *Chinese Journal of Chemical Engineering* **2009**, *17*, 150–155.

[15] Stuart, B. *Polymer Analysis*; John Wiley and Sons: Chichester, UK, 2002.

[16] Rubinstein, M.; Colby, R. *Polymer Physics*; Oxford University Press: Oxford, UK, 2002.

[17] Cohen-Addad, J. P. *NMR and Fractal Properties of Polymeric Liquids and Gels*; Pergamon Press: London, UK, 1992.

[18] Sun, S.; Chen, X.; Liu, J.; Yan, J.; Fang, Y. *Polymer Engineering and Science* **2009**, 99–103.

[19] Bunn, C. W. *Nature* **1948**, *161*, 929–934.

[20] Bhat, N. V.; Nate, M. M.; Kurup, M. B.; Bambole, V. A.; Sabharwal, S. *Nucl. Instrum. Meth.* B. **2005**, *237*, 585–592.

[21] Hoerter, M.; Oprea, A.; Barsan, N.; Weimar, U. *Sensor and Actuators* B. **2008**, *134*, 743–749.

[22] Ban, F. Y.; Majid, S. R.; Huang, N. M.; Lim, H. N. *Int. J. Electrochem. Sci.* **2012**, *7* 4345–4351.

[23] Sun, G.; Li, X.; Qu, Y.; Wang, X; Yan, H; Zhang, Y. *Materials Letters* **2008**, *62*, 703–706.

[24] Titelman, G. I.; Gelman, V.; Bron, S.; Khalfin, R. L.; Cohen, Y.; Bianco-Peled, H. *Carbon* **2005**, *43*, 641–649.